

Microclimate performance of an open atrium office building: a case study in thermo-fluid modelling

F ALAMDARI, MSc, PhD, CEng, MCIBSE
Thermo-Fluid Energy Ltd, Bath, UK.

S C EDWARDS, MSc, CEng, FCIBSE

Hoare Lea and Partners, University of Bath, Bath, UK.

S P HAMMOND, MSc, CEng, MIMechE, MInstR

School of Architecture and Building Energy, University of Bath, Bath, UK.

SYNOPSIS The design of the new headquarters for Hoare Lea and Partners, consulting engineering, coincided with the greater emphasis on energy efficient and environmentally friendly methods for engineering buildings. A naturally-ventilated atrium design was therefore adopted consisting of two two-storey buildings connected by an entrance hall, each with a central open atrium. In the present contribution a finite-volume CFD code has been used to examine the environmental performance of these offices. This case study also facilitates a better physical understanding of the sort of complex air flow patterns found within buildings of this type.

NOTATION

| | |
|-------------------|--|
| a | coefficients in discretization equations |
| C | convective term in discretization equations |
| C_μ, C_1, C_2 | constants in the k- ϵ turbulence model |
| D | diffusion term in discretization equations |
| G_k | shear generation term in the k-equation |
| g_i | gravitational vector (9.81 m s^{-2}) |
| H | enthalpy (J kg^{-1}) |
| k | turbulence kinetic energy ($\text{m}^2 \text{ s}^{-2}$) |
| S_ϕ | sources or sinks of variable ϕ |
| S'_p, S''_p | coefficients in linearised sources or sinks in discretization equations |
| t | time (s) |
| T | absolute temperature (K) |
| T_{ref} | reference temperature (K) |
| u_i | velocity components in the co-ordinate direction x_i (m s^{-1}) |
| x_i | coordinate directions (m) |

Greek Symbols

| | |
|------------------|--|
| β | coefficient of cubic expansion (K^{-1}) |
| ϕ | any dependent variable |
| Γ_ϕ | effective diffusion coefficients for each ϕ |
| ϵ | turbulence energy dissipation rate ($\text{m}^2 \text{ s}^{-3}$) |
| θ | $T - T_{ref}$ (K) |
| ρ | fluid density (Kg m^{-3}) |
| μ | dynamic viscosity ($\text{kg m}^{-1} \text{ s}^{-1}$) |
| σ | Prandtl number |
| $\alpha(Pe_n)$ | weighting function |

Subscripts

| | |
|---------|---|
| eff | effective (laminar plus turbulent) |
| p and n | central and neighbouring nodes in domain discretization grid respectively |
| ref | reference values |
| l | laminar |
| t | turbulent |

1. INTRODUCTION

1.1 The case study

Atria, or large glazed spaces, incorporated into office buildings have gained popularity within the architectural profession, both in Europe and North America, over the last decade. The original motivation for such designs were cost reduction, energy efficiency, and aesthetic considerations. However, an awareness of the potential environmental benefits of naturally-ventilated atrium buildings has more recently gained ground. An atrium can be used to induce ventilation air flow through an office complex by suitable location of inlet and extract openings. This avoids the need for air conditioning and refrigeration plant, thereby removing a potential source of CFC emissions.

The design of the new headquarters for Hoare Lea and Partners, consulting engineers, coincided with this greater emphasis on energy efficient and environmentally friendly methods for servicing buildings. A naturally-ventilated atrium design was therefore adopted for these new commercial offices located at the Aztec West Business Park on the northern outskirts of Bristol. The offices consist of two identical two-storey buildings (each 20m square in plan) connected by an entrance hall and each having a central open atrium. The atrium provides the basis of the natural ventilation system, with air flowing in at side windows, across the office space, and then being vented through automatically controlled louvres in the roof glazing. This air flow is induced by a combination of wind pressures on, and stack effect within, the building depending on the external climatic conditions. Construction of this atrium building, now known as Aztec West 140, was completed in September 1989.

1.2 Computational fluid dynamics of the built environment

There is currently an upsurge of interest in air movement and stratification within the technical community concerned with building energy and

environmental performance (1). This is not surprising in view of the growing awareness of the importance of modelling building airflow and related phenomena for performance analysis. A number of sophisticated building energy simulation programs have been developed since the mid-1970's that model the dynamic thermal behaviour of the system. However, a weakness in all these new computational approaches is that emphasis has been placed on simulating the transient performance of the building fabric, while air flow and convective heat exchange in and around the structure are modelled using only rough approximations. Furthermore, considerations of environmental quality within building spaces, which is again heavily dependent on air movement, have taken on a high profile in recent years. In addition, the adoption of some of the modern architectural features, such as atria in office complexes, gives rise to new and complex fluid dynamic problems.

It is hoped that computational fluid dynamics (CFD) modelling may eventually replace, or at least complement, the more traditional approaches to simulating building airflow. All thermo-fluid problems are governed by so-called 'conservation laws' such as those for mass, momentum, thermal energy, and species concentration. These laws can be represented mathematically by a set of complex 'elliptic partial-differential equations. In principle it is therefore possible to solve such equations for any conservation phenomenon using modern numerical techniques. This includes air, heat and smoke (or other contaminant) transport within and between the zones of naturally and mechanically-ventilated buildings. However, in practice, CFD computer codes presently have a number of limitations (1), and are costly in terms of computing resources. Consequently, simplified methods are often used, and are likely to be so for some time to come.

1.3 The problem considered

In the present study a 'field' CFD model is used to simulate the microclimate conditions within Aztec West 140. The model solves finite-volume approximations to the governing 'elliptic' conservation equations for mass, momentum and thermal energy, and is capable of representing complex, three-dimensional geometries as is required for the atrium case study. This CFD model consequently enables the indoor thermal environment to be evaluated under various, summer and winter, climatic conditions from computed distributions of, for example, air velocities and temperatures.

The present contribution therefore employs a field CFD code to examine the environmental performance of a particular atrium office building. Nevertheless this case study facilitates a better physical understanding of the sort of complex air flow patterns found within buildings of this type. In addition, comparisons with the original expectations of performance at the design stage provide a basis for making general recommendations for future use.

2. THE OPEN ATRIUM BUILDING

2.1 Background

In 1989 Hoare Lea and Partners took a bold decision and relocated their offices from the traditional location of a city centre to a newly created Arlington Business Park called Aztec West. (Aztec derived from A to Z technology.) The Aztec West business park is a campus style development on the north side of Bristol close to the M4 and M5 interchange, and some seven miles from Bristol City Centre. Hoare Lea and Partners are a long established practice (since 1862) of consulting engineers specialising in building environmental engineering and the associated mechanical and electrical engineering systems.

The practice has a number of UK offices, but the Bristol branch also accommodates the central administration department for the firm as a whole which the development at Aztec West had to accommodate together with the Bristol office personnel a total of approximately 90 persons. The space within the building of about 1300m² in total had to provide suitable flexibility of layout and office types to provide efficient working facilities for a number of uses. Individual offices were required for partners, whilst the engineering groups of about 8 persons needed open plan space to take account of engineer desks and desk top computers, drawing boards, secretarial desks and word processors. A separate computing area was also required for CAD and other centralised computing facilities such as environmental simulation, CFD evaluations and CAD with electrostatic printers.

In addition a printing room was required to provide the 'In House' printing facility for drawings specifications and reports. The central administration department required a secure and separately partitioned area to accommodate the partnership's secretary, accountant and their assistants. The partnership saw this move to Aztec West as an ideal opportunity to not only develop the building as a pleasant work place but also to rigorously assess design alternatives for both the architecture and engineering to create a refined economic, work efficient and environmentally friendly building in the well planned and landscaped business village within the park.

2.2 Conceptual design

From the outset the partners wanted to create a form for the building that addressed not only the microclimate and solar orientation but also symbolised as far as possible the partnerships 'modus operandi'. Although the development could be classified as 'green field' there was a master plan for the site as a whole and in particular the business village. The site that was available was segmented in shape with the north-south line forming two approximately equal sub-segments. Furthermore the building had to fit in with the master plan visually and there were constraints such as the ratio of car parking required at 1 car per 20m² of office space and no cars allowed to be parked on the access roads. These constraints perhaps aided the progress of the conceptual design as they provided a starting point from which to work.

The conceptual design that emerged was a

building of two storeys. For reasons of flexibility and future possible subletting of areas the building was effectively split into four lettable parts in two distinct building forms and joined by a link. Each of the two parts were provided with a two-storey open atrium incorporating louvre ventilators in the roofs. The partners as designers were keen to exploit a building design that was energy efficient and that worked with nature rather than against it.

The materials that were chosen for the walls the roof and the structure of steel and concrete had good thermal capacities providing long time lags and low decrement factors. Double glazing was used throughout and the roofs at both ground and first floor levels had overhangs to give solar shading to the windows. The designers were of a view, and calculations at the time supported this, that if the building could be naturally ventilated with copious amounts of fresh air then the somewhat deep plan of the ground floor (20m x 20m), and the galleried design for the first floor with the opening louvres in the atrium roof glazing would provide temperatures within the building that were at worst no greater than the external air temperatures. At best the 'resultant dry' temperatures within the building would be within the comfort zone for over 98% of the occupied annual period.

2.3 The detailed design

The design of the final building is illustrated in Figs. 1 and 2. The total area of the building including the link was 1320m². The construction materials chosen are given in Table 1.

The principal features of the thermal environmental engineering systems that were provided independently for the two halves of the building are given in Table 2.

The thermal requirements for the heating of the building were assessed using the Cymap suite of programmes, which dominantly use the CIBSE methods of calculations. For summer a Cymap programme was used to evaluate expected peak summer time temperatures incorporating large natural ventilation rates assessed by ASHRAE methods. The latter are induced by the large number of opening windows and the atria roof louvres. In these calculations the thermal effects from shading of the glazing by the generous 1.0 metre wide roof overhangs, and also the thermal gains from the 500 lux lighting and the 20W/m² of electrical pave were taken into account. All the east, south and west elevation windows have opening panels and are provided with manually adjustable plain calico blinds. None of the atria glazing panels are provided with blinds. The heating and ventilation systems are provided with automatic controls; the details of which are given in Table 3.

All the heating and ventilation systems were commissioned upon completion, and have been running satisfactorily since the building was occupied.

3. COMPUTATIONAL FLUID DYNAMICS MODELLING

3.1 Background

Air flow and convective heat transfer within an enclosure are governed by the principles of conservation of mass, momentum and thermal energy (or enthalpy). These 'conservation laws' may each be expressed in terms of 'elliptic' partial differential equations, the solution of which provides the basis for a field CFD model. A discretized form of the governing equations may be obtained by dividing the flow domain into a finite set of small sub-domains, each surrounding a node of the computational grid. The discretized equations are then formulated in such a way that integral conservation requirements are satisfied for individual sub-domains or control volumes. This approach has been called the 'control-volume method' by Patankar (2), and the discretized equations might preferably be distinguished by the prefix 'finite-volume', rather than the term 'finite-difference' commonly employed. The finite-volume equations are solved in the present mathematical model by methods similar to those used in the TEACH and CHAMPION family of finite-volume programs developed by Gosman and Pun (3) and Pun and Spalding (5) respectively. Both these codes employ the SIMPLE ('semi-implicit method for pressure linked equations') algorithm of Patankar and Spalding (6), but are restricted to two-dimensional geometries. Two of the present authors and their co-workers used their early experience in applying the CHAMPION code to mechanical ventilation problems (6,7) in order to develop a more general computer program capable of simulating three-dimensional flow fields (Alamdari et al (8)). This is called the ESCEAT (Elliptic Equation Solver for Convection and Heat Transfer) code, and was originally employed to compute convective heat transfer in warm-air heated rooms (9). However, this is essentially a research code, and for the present purposes a commercially developed code, FLOVENT, has been employed. It has been adopted as an exemplar of the present generation of commercial CFD codes in order to assess their utility in the context of building environmental performance analysis.

Several authors have reported field CFD model computations for three-dimensional mechanically-ventilated enclosures with both buoyant and non-buoyant conditions. Hjertager and Magnussen (9) developed a finite-volume computer code based on the SIMPLE algorithm (5) which they used to predict the flow and thermal field in a room with a high side-wall register and adjacent ceiling extracts. Buoyancy effects were introduced by way of heated panels in the floor and far wall, together with a cooled air supply. Closure of the finite-volume equations for this turbulent flow was obtained using the popular 'two-equation', 'energy-dissipation' turbulence model (Launder and Spalding (10)), an extended form of which has been adopted for the present study. The authors' comparisons with experimental data (9) displayed good agreement for the isothermal case, although not for the buoyant one. They appear to have made an allowance for buoyancy effects in the mean-flow equations, but not in the turbulence model ones. It is therefore not surprising that their computations were less satisfactory for strongly buoyant flows. A subsequent study by Sakamoto and Matsuo (11) using an early finite-difference technique examined the isothermal flow in a rectangular room with a square, ceiling-mounted supply air 'diffuser' and a low side-wall

extract. They employed two different turbulence closure approximations: the standard energy-dissipation model (10) and a more advanced 'large eddy simulation' approach. Comparison with their own experimental measurements (11) displayed fairly good agreement for the mean-flow field, although not for some of the turbulence properties. Discrepancies were equally apparent with both turbulence closure assumptions, and the authors therefore recommended the use of the simpler energy-dissipation model on grounds of computational economy. Gosman et al (12) used this model, together with a three-dimensional version of the TEACH program, to compute the isothermal flow field in a rectangular enclosure having a square high side-wall register. They report comparisons with mean-flow data that they obtained using laser-doppler anemometry in a small-scale test rig. Similar studies of recirculating flow in three-dimensional mechanically-ventilated rooms (13,14) have more recently been undertaken using finite-volume codes and the k-ε turbulence closure. Both Awbi (13) and Murakami and Kato (14) found generally good agreement between computations and albeit limited mean-flow data for high side-wall and ceiling mounted diffuser applications respectively.

3.2 Mathematical framework

The governing time-averaged elliptic equations for the turbulent flow, thermal energy and chemical species may be represented in a common form, using tensor notation (1):

$$\partial(\rho\phi)/\partial t + \partial(\rho u_j \phi)/\partial x_j = \partial\{\Gamma_\phi(\partial\phi/\partial x_j)\}/\partial x_j + S_\phi \dots\dots(1)$$

where $u_j (u_1, u_2, u_3)$ are the time-averaged (mean) velocity components in the coordinate directions $x_j (x_1, x_2, x_3)$, ϕ are any of the dependent variables, Γ_ϕ are the effective diffusion coefficients, S_ϕ are the sources or sinks, ρ is the fluid density, and t is time.

The closure of the equation set was achieved in this study by using the standard 'two-equation' models of turbulence, closure, the k-ε model (10). This model defines the isotropic 'eddy' viscosity, or turbulent exchange coefficient for momentum (μ_t), from two additional variables, the turbulence kinetic energy (k) and its dissipation rate (ε), that characterize the local state of turbulence. Mathematical expressions for the diffusion coefficient and source terms for each variable are given in Table 4.

In order to bridge the steep dependent variable gradients close to the solid surface, the FloVENT code employs the standard 'wall-functions' (10). These are simply based on the well-known bilogarithmic behaviour of the mean velocity and temperature near solid walls. The resultant velocity in planes parallel and close to any surface may therefore be obtained, which utilises conventional near-wall scaling (8) and (10).

3.3 Numerical solution procedure

The numerical simulation of the fluid flow and heat transfer equations involves the solution of

a set of coupled, non-linear partial differential equations. It requires some discretization of the flow domain into a finite set of cells, formed by computational grid. The differential equations, Equation 1, may then be integrated over each cell volume of the computation grid. This leads to a set of algebraic equations in the following finite-volume form:

$$(a_p - S'_p)\phi_p = \sum_n a_n\phi_n + S_p \dots\dots(2)$$

where, the coefficients $a_n = D_n \alpha(|Pe_n|) + [[0, \pm C_n]]$ and $a_p = \sum_n a_n$. Indices p and n denote the central computation grid point and its neighbouring points respectively, C and D indicate the strength of the convection and diffusion respectively, $\alpha(|Pe_n|)$ is a weighting function, and the symbol $[[a,b]]$, denotes the greater of a and b. In the code used in this study the weighting function is evaluated using an 'upwind' differencing scheme (2) and the source terms S_p , in Equation 1 is evaluated using a linearised expression $(S_p + S'_p\phi_p)$ in order to enhance numerical stability. The velocity components are calculated in the code at staggered locations mid-way between adjacent grid nodes (5). This practice has the advantage of ensuring that the velocities are directly available for calculating the convective fluxes of the scalar variables, as well as lying between the location of static pressures that drive them. However, it necessitates some changes to the coefficient expressions (2).

The algebraic equations, Equation 2 are solved by the code in an iterative manner, using a tri-diagonal matrix algorithm, and the velocities and pressures are calculated via the SIMPLE algorithm (5). The computational grid employed for the present simulation utilised a 29 x 17 x 30, non-uniform nodal network, whose fineness can be judged by the velocity vector diagrams presented in Fig. 4.

3.4 Geometry and Computational Grid

The first step in the solution of the algebraic finite-volume equations represented by Equation 2 is the discretization of the flow domain and the definitions of the points at which variables are located. Discretization of the flow domain must conform to the boundaries in such a way that boundary conditions can be accurately represented and allow the computational cells to be small in regions with steep property gradients. Domain discretization is provided by a computational grid generated using an appropriate coordinate system. In the current version of FloVENT (version 1.2) building spaces may be discretized by using rectangular cells (or control-volumes) and adopting simple Cartesian coordinate system. Therefore in the present contribution the geometry is modelled in a full three-dimensional Cartesian coordinate system. The coordinate axes were aligned with the walls and floor of the building. The grid distribution were non-uniform and the computational cells were concentrated in regions with high thermal and velocity gradients. Internal partitions and walls were represented by way of cell-face and control-volume blockages. However, the current version of FloVENT code geometrically provides facilities to represent the angled plates and triangular blocks, but these are restricted to frictionless

surfaces without heat transfer and adiabatic blocks. Therefore, the roof of the building was represented by 'best step-wise' fit to a grid and cuboidal blocks. This allows heat gain and heat loss through the roof in summer and winter conditions respectively, although the accuracy of the solution may be affected by the step-wise roof geometry adopted. The capability of the code and accuracy of the solution may be enhanced by the adoption of the numerical grid generated techniques, using the boundary-conforming (body-fitted) coordinate system to generate a grid to fit irregular boundaries.

4. BUILDING AIRFLOW AND ENVIRONMENTAL PERFORMANCE

4.1 Thermal boundary conditions

It is normal practice with CFD models to specify the internal thermal boundary conditions for the enclosure. These are often taken from measured surface temperatures, and therefore effectively account for (both long and short-wave) thermal radiation exchange within the space. In the case of the FloVENT program there are two alternative options. The authors chose to use the one for which it is required to specify the external (wind-induced) convective heat transfer coefficient and the wall conductivities. The former was inferred from the estimated construction U-values, and assumed values for the internal surface resistances taken from the CIBSE Guide. The alternative option was to prescribe surface temperatures, but these were not known to the authors at the time of the case study.

The heat emitters were thermostatically controlled such that they operated at full load when the external air temperature was -5°C , and were shut off when it reached $+15^{\circ}\text{C}$. Consequently, the specified heat output from the emitters was adjusted according to a linear characteristic. The locations and heat outputs of the light fittings were also specified, assuming that they were in full operation both in summer and winter. This is clearly an overestimate, but it was to some extent compensated by the fact that no allowance was made for the heat output of other electrical devices, such as desk top computers.

4.2 Winter simulation and observations

The winter simulations were carried out for a typical outside air temperature of $+1^{\circ}\text{C}$ on a notionally calm day. Computed results are presented in Figs. 4-7 with both velocity vector plots and temperature distributions shown. Despite the relatively cold weather conditions the minimum temperatures in occupation zones were computed to be 20°C . A maximum temperature of 28°C is computed in the open plan office opposite the entrance hall. In reality these high temperatures would not occur as the perimeter heaters in hot zones would locally control the emitter. The occupants also have the facility to open windows to increase the local ventilation rate. It was necessary (at least initially) to assume for the CFD simulation that the perimeter heaters were globally controlled, and that all the windows were closed. These restriction could be removed for subsequent computations if desired.

Under winter conditions the roof vents above the open atrium remain closed. Consequently air movement in winter is induced largely by internal buoyant plume emanating from the heat emitters located around the perimeter on each floor. Air velocities are therefore modest, with everywhere being less than 0.25 ms^{-1} , but sufficiently high to avoid the sensation of stuffiness.

The thermal comfort conditions throughout the building in winter have been observed to be excellent with no cold spots, down draughts or cold radiation effects. There is no doubt that the under window high quality perimeter natural convectors with their significant radiation component contribute significantly to this good performance. It is worth emphasising specifically that the atria glazing does not cause any discomfort in winter either due to cold radiation or downward convection.

In winter external temperatures of -3°C have been experienced and no condensation has appeared anywhere on the construction materials or the non-thermally broken aluminium window frames.

4.3 Summer simulation and observations

The computations under summer conditions were performed for an external air temperature of 26°C again for a notionally calm day. Heat gain would therefore induce the roof vents to open fully. This induces air flow from the perimeter upwards through the central open atrium, and then out through the vents. Such a pattern is clearly reflected in the computed results shown in Figs. 8-11. Local velocities are consequently rather high than in winter, although still acceptable within occupation zones. Temperatures are also high, due to the fact that all the windows were assumed closed. This is an artificial case as in normal operation some of these windows will be open, inducing a higher through-flow, and thereby reducing the internal air temperatures to acceptable levels.

Site measurements on a bright evening with an external air temperature of 16°C and a moderate breeze, indicated that the ground floor work space and library/atrium areas exhibited air temperatures of 21 and $22\frac{1}{2}^{\circ}\text{C}$ respectively. The corresponding temperatures on the open areas of the first floor were about 24°C . This is consistent with the computed temperature distributions at an elevated outside air temperature.

External temperatures of $+35^{\circ}\text{C}$ have been experienced in summer. The internal temperatures were in the warmest places with the building within 1°C of the external temperature with all the windows and all the atria roof louvres open. An unexpected benefit with the atria roof louvres has been that not only does the warm air pass out through the louvres in summer, but that there is a definite inflow of some fresh air that reaches all the way to the office areas at the bases of the atria.

An unexpected disadvantage of the ground floor roof and its overhang is that on sunny days when the slates of the roof are exposed to solar radiation, absorption and convection from the

slates occurs and on the South and West elevations in particular the convected warm air off the slates can pass directly into the open first floor windows.

5. CONCLUDING REMARKS

The design of the new headquarters for Hoare Lea and Partners coincided with the greater emphasis on energy efficient and environmentally friendly methods of engineering buildings. A naturally-ventilated atrium was therefore adopted consisting of two separate two-storey buildings connected by an entrance hall, each with a central open atrium. The staff occupying the buildings are almost unanimous in the view that the building with its form of heating and generous opening windows with atria roof louvres, is a comfortable and efficient workplace for over 95% of the time.

In the present contribution a finite-volume CFD code has been used to examine the environmental performance of the above offices. Several lessons may be drawn from the computations reported here. Firstly, it is evident that such models are capable of simulating the complex flow patterns generated within the building. Accurate prediction of the flow and thermal field are needed in order to determine, for example, the occupation zone thermal comfort conditions. The results of the present study have illustrated the desirability of the CFD modeller and the environmental engineering designer working together in an iterative manner. In this way realistic thermal boundary conditions can be developed for the model, and improved simulations obtained. Some further development is desirable on the evolution of flexible computational meshes that can adapt to the sort of complex geometries found in modern office buildings.

The partners of Hoare Lea have decided to air condition a west facing conference room to provide resultant dry temperatures in summer of no more than 23°C. A novel system is being installed using a combination of displacement ventilation and chilled beams with cool water (13°C) being generated by a chiller/ice store combination. The air movement within the conference room may well be examined using a CFD model of the type used in the present study.

ACKNOWLEDGEMENTS

The authors are grateful to Richard George, Nick Organ and Terry Wyatt of Hoare Lea and Partners for helpful discussions concerning the thermal environmental design and performance of Aztec West 140. The work reported here was partially supported by Science and Engineering Research Council grant GR/D/8042.1 awarded to the third author (Professor Hammond). He would also like to acknowledge the support of British Gas plc, who sponsor his Chair.

The authors' names appear alphabetically

REFERENCES

(1) HAMMOND, G.P., Modelling building airflow and related phenomena, BEPAC meeting Papers, December 1988 (Building Environmental Performance Analysis Club, BRE, Watford).

- (2) PATANKAR S.V., Numerical Heat Transfer and Fluid Flow, 1980 (Hemisphere, Washington).
- (3) GOSMAN, A.D., and PUN, W.M., Calculation of Recirculating Flows, Imperial College (London Univ.) Mech. Eng. Dept. Report HTS/74/2 1974 (Second Edition).
- (4) PUN W.M. and SPALDING, D.B., A General Computer Program for Two-dimensional Elliptic Flows, Imperial College (London Univ.) Mech. Eng. Dept. Report HTS/76/2, 1976 (Amended 1977).
- (5) PATANKAR S.V. and SPALDING D.B., A calculation procedure for heat, mass and momentum transfer in three-dimensional parabolic flows, Int. Journal of Heat and Mass Transfer, 1972, 15, 1787-1806.
- (6) ALAMDARI, F., HAMMOND G.P. and MELO C. 'Appropriate' calculation methods for convective heat transfer from building surfaces, Proc. First UK National Heat Conf., Leeds, 1984, 2, 1201-1211 (I.Chem.E/Pergamon, Oxford)
- (7) ALAMDARI, F., HAMMOND G.P. and MONTAZERIN N., Heat/mass transfer beneath a two dimensional wall-jet deflected by a normal, flat plate obstruction, Heat transfer 1986: Proc 8th Int. Heat Transfer Conf., San Francisco, 1986 3, 1213-1218 (Hemisphere, Washington)
- (8) ALAMDARI, F., HAMMOND G.P., and MOHAMMAD W.S., Computation of air flow and convective heat transfer within space-conditioned, rectangular enclosures, Proc. CIB 5th Int. Symp. "Use of Computers for Environmental Engineering Related to Buildings", Bath, 1986, 191-205 (CIB/CIBSE, London)
- (9) HJERTAGER B.H. and MAGNUSSEN B.F., Numerical prediction of three-dimensional buoyant flow in a ventilated room, Heat Transfer and Buoyant Convection, 1972, 2, 429-441 (Hemisphere, Washington)
- (10) LAUNDER B.E. and SPALDING D.B., The numerical computation of turbulent flows, Computer Methods in Appl. Mech. and Eng., 1974, 3, 269-289.
- (11) SAKAMOTO Y. and MASKSUO Y., Numerical predictions of three-dimensional flow in a ventilated room using turbulence models, Appl. Math. Modelling, 1980, 4, 67-72.
- (12) GOSMAN A.D., NIELSEN P.V., RESTIVO A. and WHITELOW J.H., The flow properties of rooms with small ventilation openings, ASME J. Fluids Eng., 1980, 102, 317-323.
- (13) AWBI, H.B., Application of computational fluid dynamics in room ventilation, Building and Environment, 1989, 24, 73-84.
- (14) MURAKAMI, S., and KATO S., Numerical and experimental study on room airflow: 3-D predictions using the k- turbulence model, Building and Environment, 1989, 24, 85-97.

Table 1 Construction Materials

| Element | Materials | U-Value W/m ² K |
|--------------------|---|----------------------------|
| Ground floor walls | 100 Beare Green brick 50 cavity, 25 Thermofoil insulation, 100 Thermalite block, 13 plaster | 0.44 |
| First floor walls | 13 laminate panel, 50 cavity, 25 Thermofoil insulation, 1 150 Thermalite block, 13 plaster | 0.45 |
| Glazing | Hermetically sealed panels with aluminium frames | |
| Ground floor | Solid concrete | 0.66 |
| First floor | 150 concrete on profiled metal permanent shuttering with suspended ceiling and raised floor | - |
| Roof | Slates, sarking felt, 25 Thermofoil insulations, Timber on steel structure, 25 ribbed fibre board ceiling | 0.60 |

Table 2 Thermal Environmental Engineering Systems

| Element | Description (each half of the building) |
|-------------------------------|--|
| Heating system | Gas fired Streibel 96kW Bicalor boiler generating LTHW at 82°C/72°C supplying Zehnder perimeter natural convectors sited beneath windows in the office spaces and in the office spaces. In the link Runtal high level heaters. |
| Natural ventilation system | <ul style="list-style-type: none"> i) opening perimeter windows double glazed manufactured by Planet with aluminium frames but without thermal breaks ii) Four opening roof glazed motorised louvres each 1700 x 1400 thermostatically controlled, manufactured by NUAIRE. |
| Mechanical ventilation system | Extract ventilation provided in each of the system WC areas powered by NUAIRE extract fans |

Table 3 Thermal Environmental Controls

| System | Automatic Control |
|-------------------------------|---|
| Boilers | Gas fired boilers by control and limit thermostats to provide LTHW at 82°C. Time switch controlled from Landis and Gyr's microprocessor. Domestic hot water generated from the 'in built calorifier' of the boiler and controlled at 65°C. |
| Heating system | Weather compensated with office space temperature override to control the LTHW flow and return temperature between -3°C at 82°C and 15°C at 20°C using the microprocessor. Frost override incorporated. Each of the heat emitters under the windows provided with a thermostatic flow control valve. The valence heaters in the link provided with an independent grouped local temperature controller. |
| Natural ventilation system | Opening roof glazed motorised louvres system provided with temperature controlled actuators to open when temperatures exceed chosen value. Rain sensors provided to override and open louvres in the event of fire. Whole system provided with power back up and interlinked with heating system so that louvres cannot open under temperature control if the heating system is required to be running. |
| Mechanical ventilation system | Extract fans for the WC ventilation areas time switch controlled. |

Table 4 Diffusion Coefficients and Source Terms in the Governing Equations

| Conserved Property | ϕ | Γ_ϕ | S_ϕ |
|-------------------------------|------------|-----------------------------|--|
| Mass (continuity) | 1 | 0 | 0 |
| Direction-i momentum | u_j | μ_{eff} | $-\partial p/\partial x_i + \partial/\partial x_j \{ \mu_{eff} (\partial u_j/\partial x_i) \} - \rho g_i \beta \theta$ |
| Thermal energy | H | μ_{eff}/σ_{eff} | 0 |
| Turbulence kinetic energy | k | μ_{eff}/σ_k | $G_k - \rho \epsilon$ |
| Turbulence energy dissipation | ϵ | $\mu_{eff}/\sigma_\epsilon$ | $\epsilon/k (C_1 G_k - C_2 \rho \epsilon)$ |

Notes

- $\mu_{eff} = \mu_l + \mu_t = \mu_l + C_\mu \rho k^2/\epsilon$; $\sigma_{eff} = \mu_{eff}/(\mu_l/\sigma_l + \mu_t/\sigma_t)$
- $G_k = \mu_t \partial u_i/\partial x_j \{ \partial u_j/\partial x_i + \partial u_i/\partial x_j \}$
- $\theta = T - T_{ref}$
- Constant values for turbulence mode:
 $C_\mu = 0.09$, $C_1 = 1.43$, $C_2 = 1.92$, $\sigma_l = 0.90$, $\sigma_k = 1.00$ and $\sigma_\epsilon = 1.314$



EAST ELEVATION

Fig 1 Cross-section illustration of Aztec West 140

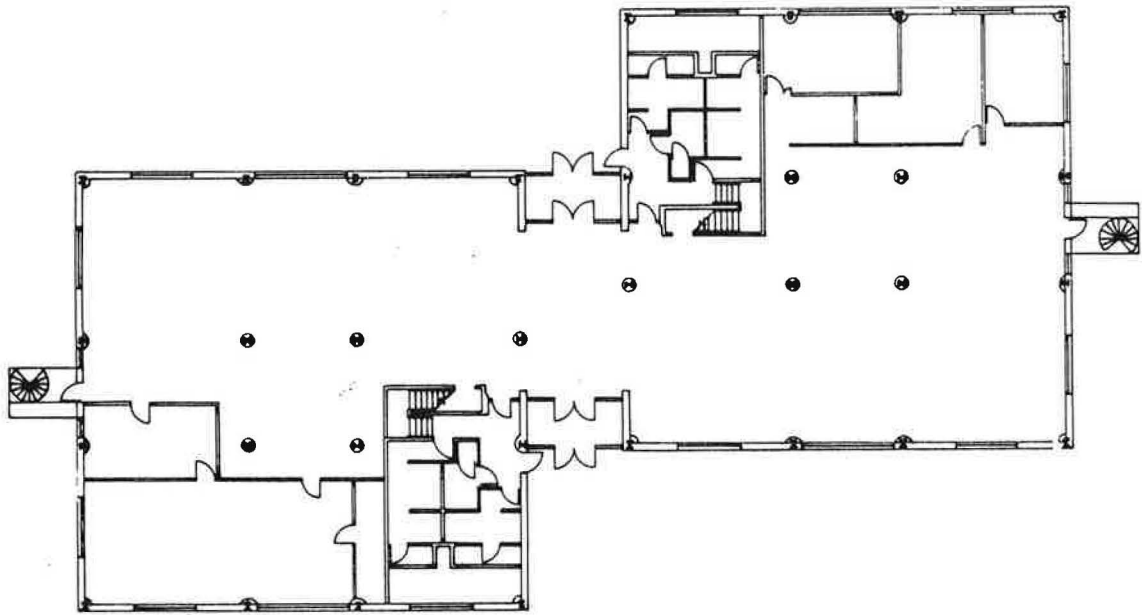


Fig 2 Ground floor plan of Aztec West 140



Fig 3 First floor plan of Aztec west 140

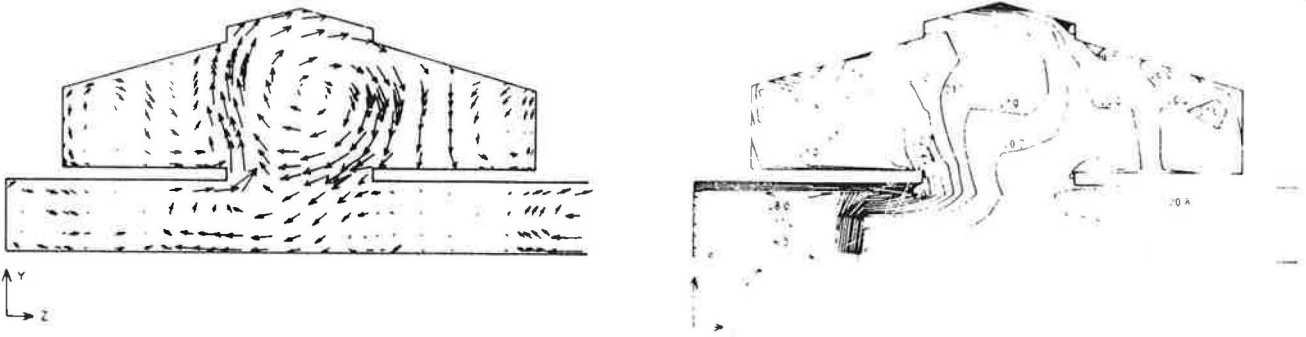


Fig 4 Winter simulation: Cross-section through entrance hall (LHS – velocity vectors; RHS – temperature field)

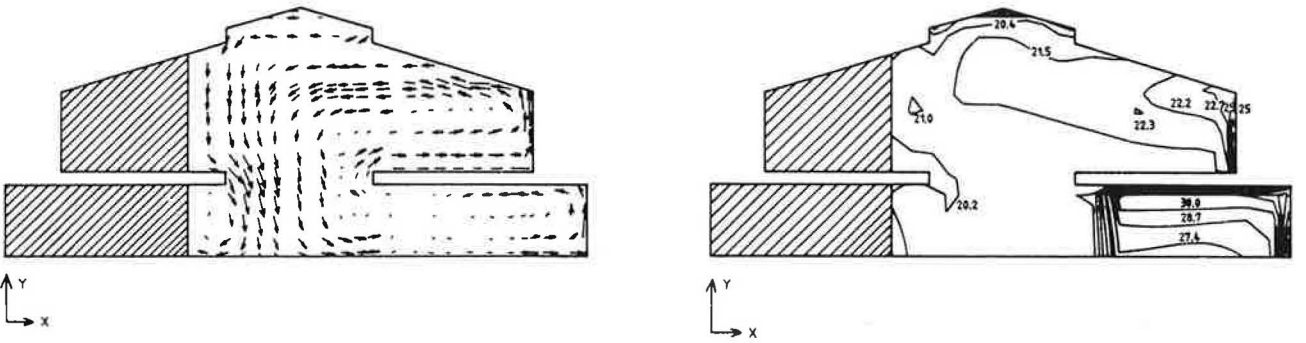


Fig 5 Winter simulation: transverse cross-section (LHS – velocity vectors; RHS – temperature field)

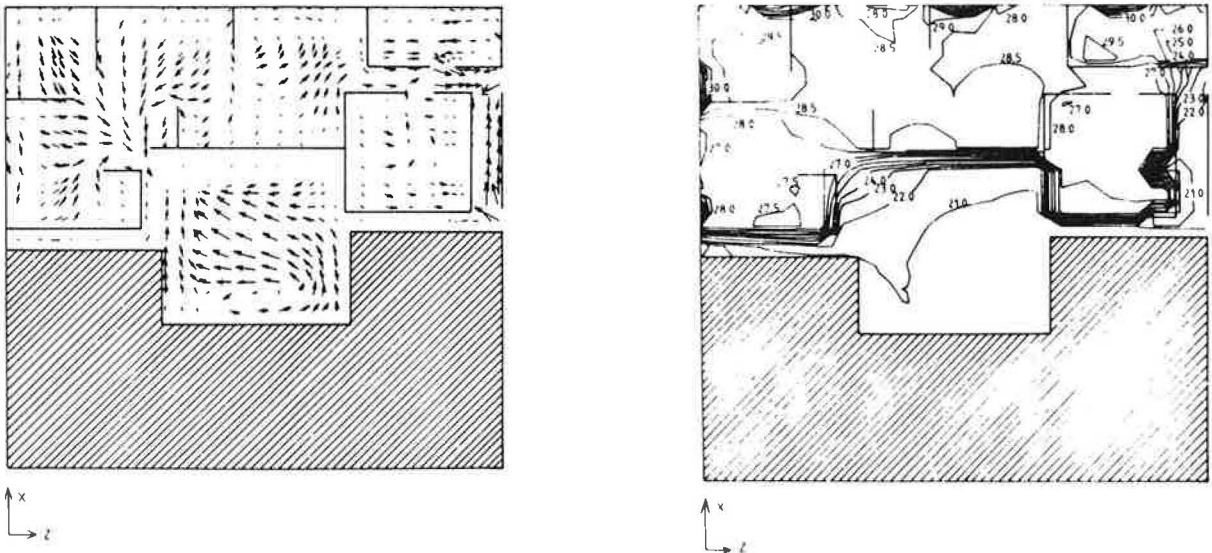


Fig 6 Winter simulation: ground floor level (LHS – velocity vectors; RHS – temperature field)

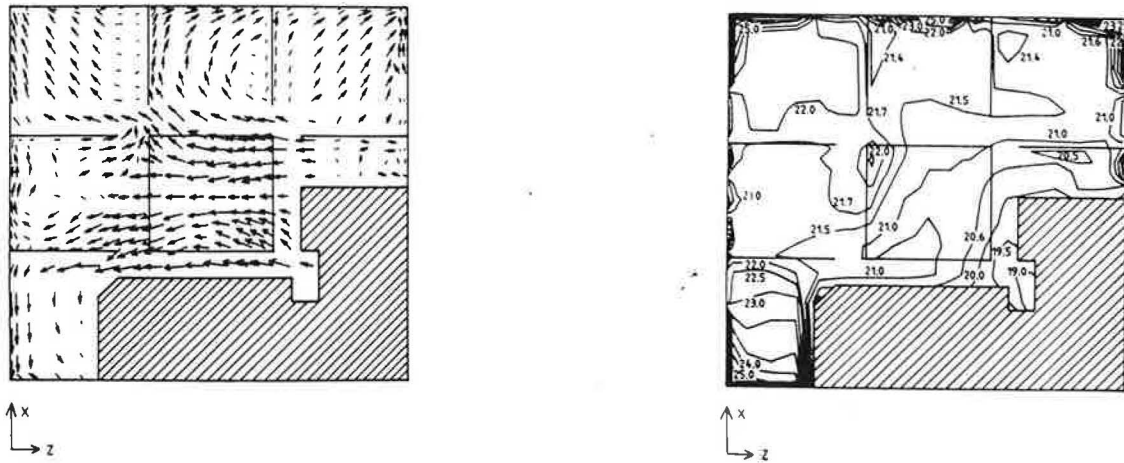


Fig 7 Winter simulation: first floor level (LHS – velocity vectors; RHS – temperature field)

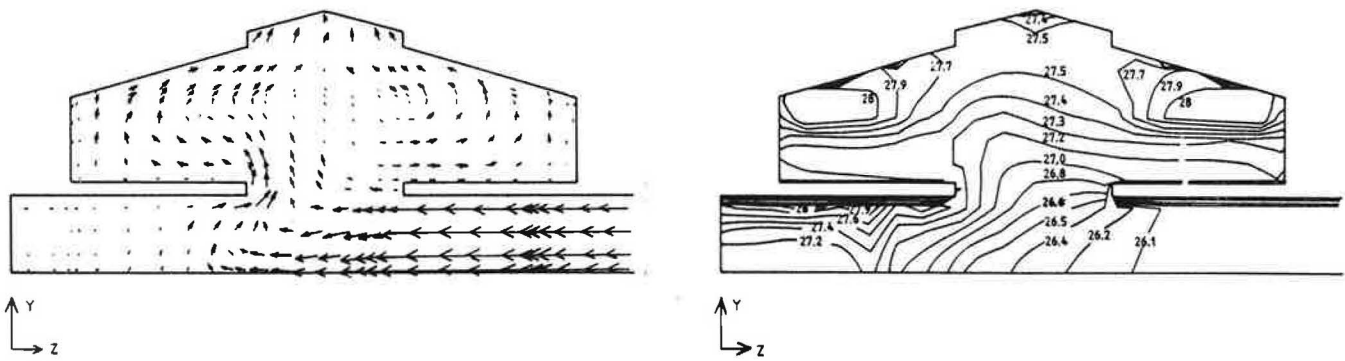


Fig 8 Summer simulation: cross-section through entrance hall (LHS – velocity vectors; RHS – temperature field)

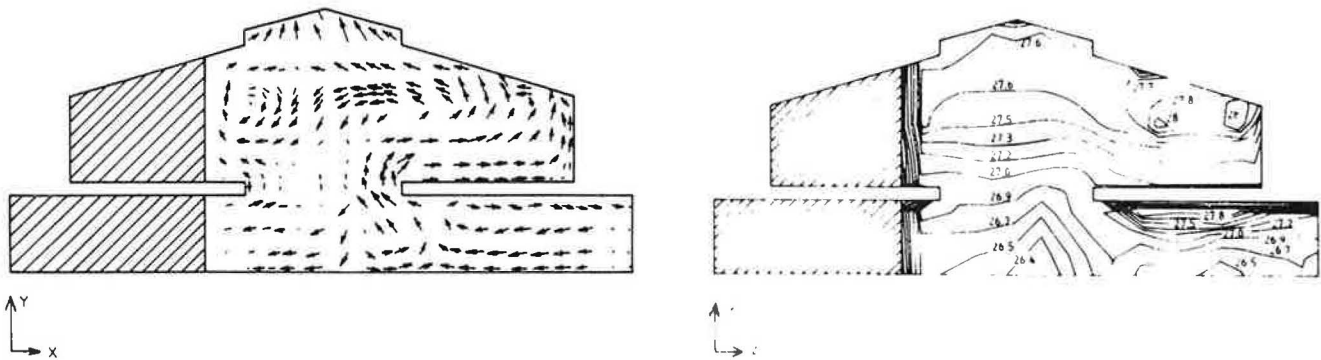


Fig 9 Summer simulation: transverse cross-section (LHS – velocity vectors; RHS – temperature field)

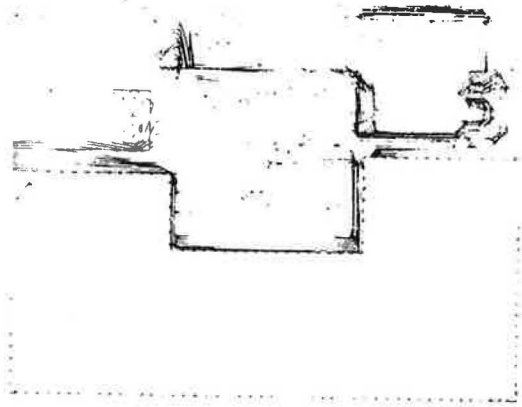
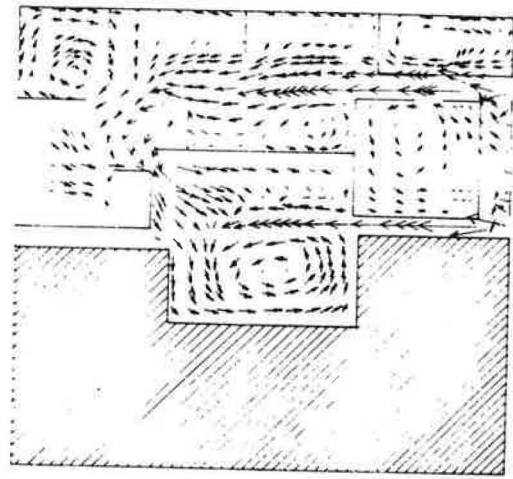


Fig 10 Summer simulation: ground floor level (LHS – velocity vectors; RHS – temperature field)

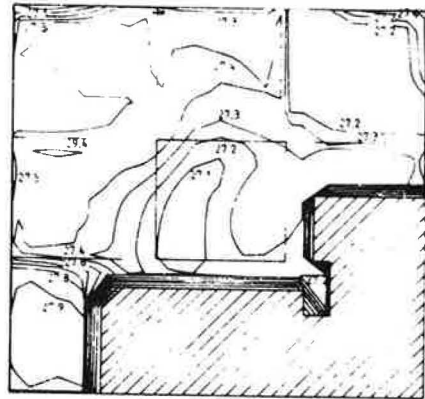
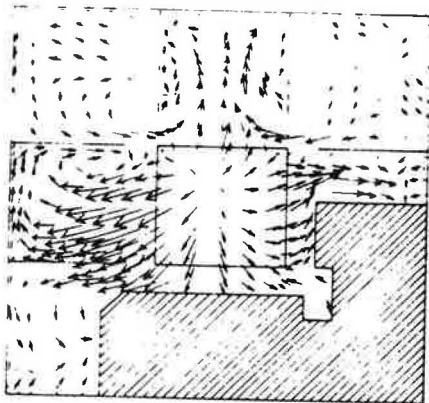


Fig 11 Summer simulation first floor level (LHS – velocity vectors; RHS – temperature field)